

International Journal of Pattern Recognition
and Artificial Intelligence

Vol. 31, No. 11 (2017) 1757006 (25 pages)

© World Scientific Publishing Company

DOI: 10.1142/S0218001417570063



1

5

7 Automatic Retinal Image Registration Using Blood Vessel 9 Segmentation and SIFT Feature

11 Fan Guo*, Xin Zhao[†], Beiji Zou[‡] and Yixiong Liang[§]

13 *School of Information Science and Engineering
Central South University, Changsha, P. R. China*

15 *Joint Laboratory of Mobile Health
Ministry of Education and China Mobile
Changsha, P. R. China*

17 *Center for Ophthalmic Imaging Research
Central South University
Changsha, P. R. China*

19 *gufancsu@163.com
†491498408@qq.com
‡bjzou@csu.edu.cn
§yxliang@csu.edu.cn

23 Received 7 January 2017

Accepted 23 March 2017

Published

25

27 Automatic retinal image registration is still a great challenge in computer aided diagnosis and screening system. In this paper, a new retinal image registration method is proposed based on the combination of blood vessel segmentation and scale invariant feature transform (SIFT) feature. The algorithm includes two stages: retinal image segmentation and registration. In the segmentation stage, the blood vessel is segmented by using the guided filter to enhance the vessel structure and the bottom-hat transformation to extract blood vessel. In the registration stage, the SIFT algorithm is adopted to detect the feature of vessel segmentation image, complemented by using a random sample consensus (RANSAC) algorithm to eliminate incorrect matches. We evaluate our method from both segmentation and registration aspects.
33 For segmentation evaluation, we test our method on DRIVE database, which provides manually labeled images from two specialists. The experimental results show that our method achieves 0.9562 in accuracy (Acc), which presents competitive performance compare to other existing segmentation methods. For registration evaluation, we test our method on STARE database, and the experimental results demonstrate the superior performance of the proposed method, which makes the algorithm a suitable tool for automated retinal image analysis.

35
37
39 *Keywords:* Retinal image; image registration; vessel segmentation; bottom-hat transformation;
SIFT feature.

41

[†]Corresponding author.

F. Guo et al.

1 1. Introduction

3 Retinal image registration is an important issue in the field of pattern recognition
5 and artificial intelligence. There are many circumstances in which registration al-
7 gorithm of retinal images is needed, such as diagnosing or monitoring retinal ab-
9 normality, etc. Two fundamental tasks in retinal image analysis (retinal image
11 segmentation and registration) are discussed in this paper. Blood vessel segmen-
13 tation for retinal image is very useful for detecting eye diseases such as glaucoma and
15 diabetic retinopathy.¹⁸ Retinal image registration is used to establish a pixel-to-pixel
17 correspondence between two retinal images.²⁴ Some image processing techniques are
19 involved in these two tasks to detect blood vessels and further generate image fea-
21 tures. Through these features, the proposed method can automatically recognize the
23 matched keypoints and finally mosaic two input retinal images. Therefore, the
25 method can be incorporated into medical expert system or intelligent computer-
aided system to help screen and diagnose ophthalmologic diseases.

17 The study of the retinal image registration is very important and necessary. The
19 main factors that will cause the difference between retinal images are⁵: (1) change of
21 eye positions including movements along X-, Y- and Z-axis; (2) change of camera
23 interior parameters, such as focal length and resolution; (3) change of imaging mo-
25 dality; and (4) change of retinal tissue in the progression of diseases. All these factors
27 make the issue of retinal image registration a hard task. Besides, due to the limitation
29 of image capture angle, the imaging regions are obtained each time always relatively
31 smaller compared to the whole fundus images. Thus, it is important to mosaic lots of
33 retinal images together, with which the doctor can achieve full information of eye
35 diseases.

25 This paper presents a new registration method for retinal images by using blood
27 vessel segmentation and scale invariant feature transform (SIFT) feature. The
29 algorithm first enhances input retinal images in the preprocessing phase and then
31 segments the blood vessels by using the bottom-hat transformation. To detect fea-
33 tures of vessel segmentation, an SIFT algorithm^{23,30} is used since it is invariant to
35 rotation, scaling and noise. Then initial matching is obtained using Euclidean dis-
37 tance, and incorrect keypoint matching is eliminated by random sample consensus
39 (RANSAC) algorithm.⁹ Although the individual technique used in both segmenta-
41 tion and registration stages is mostly known, the novel aspect of the proposed
method is in the way these techniques are combined for the retinal images, and the
results appears to be quite successful. Experimental results from both public databases
and real captured retinal images show that the proposed algorithm can reduce the
error matches and achieve good mosaic effect during the image registration process.

25 The paper is organized as follows. In Sec. 2, the related works about retinal image
27 segmentation and registration are reviewed. Section 3 describes the proposed algo-
29 rithm in details. Experimental results of the proposed algorithm on the public image
31 database are discussed in Sec. 4. In Sec. 5, we discuss some critical issues related to
33 the proposed algorithm and conclude the paper.

*Automatic Retinal Image Registration Using Blood Vessel Segmentation and SIFT Feature*1 **2. Related Works**3 **2.1. Retinal image segmentation**

5 Generally speaking, the segmentation algorithms can be divided into the unsupervised
7 and supervised methods. Unsupervised methods include matched filtering,
9 morphological processing, vessel tracking, multi-scale analysis, and model-based
11 algorithms. Many researchers use the matched filtering method to segment blood
13 vessel of retinal images. For example, Singh *et al.*³⁸ propose a matched filter approach with the Gumbel probability distribution function as its kernel to improve
15 the performance of retinal blood vessel segmentation. Mathematical morphology
17 combined with curvature evaluation⁴⁸ and centerline detection^{29,11} is used to segment
19 retinal vessel. Vessel tracking method³⁵ is also used for segmenting a vessel
21 between two points using local information. Recently, the multi-scale approaches
23 which based on scale-space analysis have drawn the attention of many researchers.
25 For example, Frangi *et al.* examine the multi-scale second-order local structure of an
27 image (Hessian) and obtain a vesselness measure by eigenvalue analysis of the
29 Hessian.¹⁰ Dai *et al.*⁶ propose a multi-scale line filter which is integrated with phase
31 congruency to detect the network of vessels in retinal images. Masoomi *et al.*²⁶ use
33 multi-scale line detection and nonsubsampled contourlet transform to automatically
35 extract blood vessels from color retinal images. The model-based approaches include
37 the vessel profile models,²⁰ active contour models,¹ graph-cut models⁴⁵ and geometric
39 models based on level sets.⁴² Different from the above unsupervised methods, the
41 supervised methods use ground truth data to classify vessels based on certain given
 features. For example, Niemeijer *et al.*³² extract a feature vector for each pixel that
 consists of the Gaussian and its derivatives at multiple scales, and then estimated the
 probability of the pixel belonging to a vessel by using a K-nearest neighbor algorithm.
 Staal *et al.*⁴⁰ present a vessel segmentation system based on the extraction of
 image ridges. Ricci and Perfetti³⁶ propose a retinal vessel segmentation method
 based on line operators. Two orthogonal line detectors along with the grey level of
 the target pixel were employed to construct a feature vector for supervised classifi-
 cation using a support vector machine (SVM). You *et al.*⁴⁶ use the complex wavelet
 followed by calculating the line strength to compute the feature vector, and the SVM
 is employed for pixel classification. Nowadays, the artificial neural network (ANN)-
 based method has achieved both scientific and economic success. For example,
 Nandy *et al.*³¹ propose an automated segmentation scheme of retinal vasculature
 using Gabor filter and ANN. Ceylan *et al.*³ propose a method for automatic blood
 vessel extraction from a retinal image using complex wavelet transform and complex-
 valued ANN. Ding *et al.*⁷ adopt an ANN-based segmentation algorithm for retinal
 vessel delineation. Li *et al.*²¹ present a cross-modality learning method for vessel
 segmentation in retinal images. The method uses a wide and deep neural network
 with strong induction ability to model the transformation. However, although good
 segmentation accuracy (Acc) can be obtained in a classifier trained by an ANN, a
 relatively long time is needed in the training phase for the ANN-based method.

F. Guo et al.

1 **2.2. Retinal image registration**

The registration methods can be divided into feature-based methods, gradient methods, and correlation methods.^{4,25} Feature-based methods manually or automatically select salient and distinctive objects, such as edge and corner, to estimate the transformation between image pair. Gradient methods estimate the translation parameters using linear partial difference equations. Since phase correlation method identifies the translation from the normalized cross-spectrum according to Fourier shift property, scaling and rotation can be estimated by using the polar Fourier representation.¹⁷ Therefore, some reliable features can be used in retinal image registration.³⁴ Generally, there are many categories of feature-based methods, such as region-matching, point-matching and structure-matching categories. The region-matching methods identify the transformation parameters by minimizing the similarity indexes. For this category, Matsopoulos *et al.*²⁸ propose global optimization-based retinal image registration scheme, and the cost function used in the scheme is defined as the error between two binary vessel images with various transformation models. The similarity index adopted in the method of Ritter *et al.*³⁷ is defined as the entropy-based mutual information. Ghassabi *et al.*¹³ propose a new structure-based region detector, which identifies stable and distinctive regions, to find correspondences. Meanwhile, a retinal fundus image registration framework can be described by the region detector. Since the region-matching methods search all the features in a region, thus the disadvantages of the methods are their huge searching space. Point-matching methods are also frequently used in image registration. The methods rely on the matched features in both input images to mosaic them. Thus, two key steps included in the methods are: feature matching and transformation estimation. The correspondence between two feature sets is established in the feature matching process. Then the transformation parameters can be identified easily and accurately as long as the matched feature pairs are reliable. For example, Zana *et al.*⁴⁷ use vessels detection and Hough transform to extract features and realize the multimodel registration of eye fundus images. Laliberté *et al.*¹⁹ impose transformation to the combination of feature points in order to search the minimal error. However, the algorithm speed depends on the number of feature points, if the feature points increases, the search will become very time-consuming. Li *et al.*²² use rotation-invariant distance instead of Euclid distance to match the SIFT vectors associated with the key feature points. The experimental results show that much more correct matches are obtained by the method since the rotation-invariant distance is independent of the main orientation of the key feature points. Patankar *et al.*³³ propose an algorithm for registration of retinal images using orthogonal moment invariants as features for determining the correspondence between the dominant points (vessel bifurcations) in the reference and test retinal images. In the method proposed by Wang *et al.*,⁴⁴ multi-feature attributes are used to guide the feature matching to identify inliers (correct matches) from outliers (incorrect matches). A probability deformable mixture model which consists of Gaussian components for inliers and

Automatic Retinal Image Registration Using Blood Vessel Segmentation and SIFT Feature

uniform components for outliers is constructed in the method. Matsopoulos *et al.*²⁷ use the self-organizing maps (SOM) to realize multimodal registration of retinal images. The method has three steps: the vessel centerline detection and extraction of bifurcation points, the automatic correspondence of bifurcation points in the two images using a SOM, and the extraction of the parameters of the affine transform. The algorithm shows good performance in Acc. However, the branching angles of single bifurcation point are the determining factor for the above methods, and the angles may easily cause matching errors in the image registration process.⁴³ Structure-matching methods mainly use bifurcation structure for retinal image registration. For example, the bifurcation structure in the method of Chen *et al.*⁴ is composed of a master bifurcation and its three connected neighbors. Once the vasculature pattern is well segmented, the error matches can be greatly reduced for retinal image registration.

15 3. Proposed Algorithm

17 3.1. Algorithm framework

The basic idea of our algorithm is to segment retinal blood vessel from the input retinal images, and then map and geometrically align the two retinal images using the segmented blood vessel. To detect features of the blood vessel images, a SIFT algorithm is adopted for this purpose.

Figure 1 depicts the algorithm framework of our vessel segmentation system. As can be seen in the figure, the proposed algorithm is divided into four major steps. The first step is to obtain enhanced input retinal images by using the guided filter¹⁵ in the preprocessing phase.

The second step is to segment blood vessel from the enhanced retinal images by using the bottom-hat transformation since the bottom-hat transformation encodes information on local intensity structure and image morphological property.

In the third step, a SIFT algorithm³⁰ is used to detect features since SIFT feature is invariant to rotation, scaling and noise. However, only SIFT algorithm can't achieve a perfect registration result, and many incorrect keypoint matching exists because of the influence from background and computation precision.

In the last step, some error matches are eliminated by using the RANSAC algorithm.⁹ The experimental results demonstrate the effectiveness of the proposed algorithm.

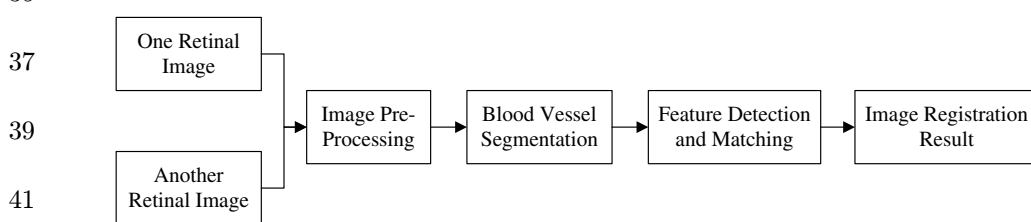


Fig. 1. Our retinal image registration framework.

F. Guo et al.

1 **3.2. Image preprocessing**

3 In the preprocessing phase, the guided filter algorithm¹⁵ is used here to enhance the
 5 input retinal images. Specifically, for the input image, it is assumed that enhanced
 7 retinal image is a linear transform of the input (guidance) image $I(\mathbf{x})$ in a window ω_x
 9 centered at pixel $\mathbf{x} = (x, y)$.

$$7 \quad \hat{I}(\mathbf{x}) = a_x^T I(\mathbf{y}) + b_x, \quad \forall \mathbf{y} \in \omega_x, \quad (1)$$

9 where a_x and b_x are linear coefficients assumed to be constant in ω_x . To make the
 11 difference between the output $\hat{I}(\mathbf{x})$ and the input $I(\mathbf{x})$ as small as possible, we
 13 minimize the following cost function in the local window ω_x centered at pixel \mathbf{x} ,

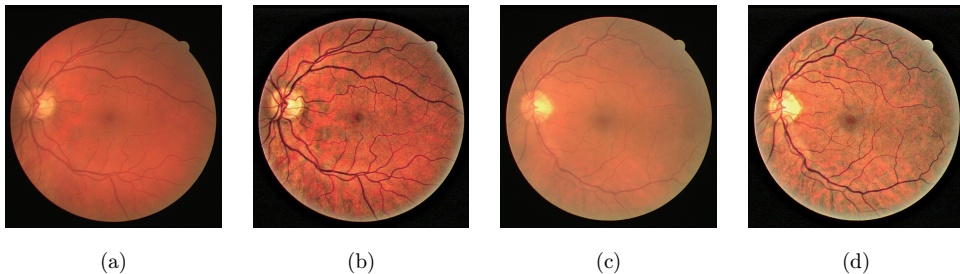
$$13 \quad E(a_x, b_x) = \sum_{\mathbf{y} \in \omega_x} \left((a_x^T I(\mathbf{y}) + b_x - I(\mathbf{x}))^2 + \varepsilon a_x^2 \right). \quad (2)$$

15 The small variable ε is a regulation parameter to prevent ω_x from being too large.
 17 The solution to (2) is given by

$$17 \quad a_x = \left(\sum_x +\varepsilon U \right)^{-1} \left(\frac{1}{|\omega|} \sum_{\mathbf{y} \in \omega_x} I(\mathbf{y})^2 - u_x^2 \right), \quad (3)$$

$$21 \quad b_x = u_x - a_x^T u_x, \quad (4)$$

23 where \sum_x is a 3×3 covariance matrix of $I(\mathbf{x})$ in ω_x , U is a 3×3 identity matrix, u_x
 25 is the mean vector of the input image $I(\mathbf{x})$ in the window ω_x . By substituting (3) and
 27 (4) into (1), we get the enhanced retinal image $\hat{I}(\mathbf{x})$. Some enhancement results are
 29 shown in Fig. 2. Note that the guided filter will not only enhance blood vessel, but
 31 also enhance image noise. However, the two input retinal images can still be correctly
 33 aligned. The high Acc of the proposed method appears mainly due to two reasons:
 35 first, the proposed method segments the blood vessel of retinal images to extract
 37 SIFT feature. Therefore, whether the blood vessels can be successfully segmented
 39 determines the quality of feature points' extraction. By using the guided filter, the
 41 blood vessels in the enhanced retinal images are more obvious than those in the
 original input images, which make it much easier for identifying the feature and



41 Fig. 2. Image preprocessing results. (a) and (c) are original input retinal image. (b) and (d) are the
 enhanced results obtained by using guided filter.

Automatic Retinal Image Registration Using Blood Vessel Segmentation and SIFT Feature

1 structure of blood vessel in the following steps. This outcome constitutes one of the
 3 method's key advantages; second, the contrast between image background and blood
 5 vessel is larger than the contrast between background and image noise, and the next
 7 step mainly uses the contrast difference to brighten the vessels. Therefore, the noise
 has little influence on the vessel segmentation results. Even if some noise is enhanced
 at the same time, the blood vessels can still be correctly segmented by using the
 proposed method.

9

3.3. Bottom-hat transformation

11 For the vessel segmentation phase, the bottom-hat transformation is used here for
 13 eradicating bright lesions. Since the green channel has a higher contrast between the
 15 vessels and the background than other channels, were the image features that
 obtained by bottom-hat transformation are extracted from the green channel of the
 17 enhanced RGB colored retinal image obtained using the guided filter for pre-
 19 processing. Bottom-hat transformation is a kind of morphological transformation. If
 21 the intensity values in a gray-level image are thought of as elevations, then a scene is
 composed of mountain tops (brightest points) and valley lows (darkest regions). The
 uneven contrast in an image will often degrade threshold isolation of adjacent
 23 mountain tops between valleys. Since the intensity of blood vessel is generally lower
 than that of background, the bottom-hat transformation is used to extract feature
 vector. This transformation can be written as^{2,12}

$$I_{th}^{\theta} = (I \cdot S_e^{\theta}) - I, \quad (5)$$

25

$$Is_{th} = \sum_{\theta \in A} I_{th}^{\theta}, \quad (6)$$

29

31 where “ I_{th}^{θ} ” is the bottom-hat transformed image, “ S_e ” is the structuring elements
 33 for morphological closing, “ I ” is the image to be processed, “.” and “ θ ” is the angular
 35 rotation of the structuring element. If the closing along a class of linear structuring
 37 elements is considered, and the length of the structuring elements is larger enough to
 extract the vessel with the largest diameter, the sum of bottom-hat along each
 39 direction will brighten the vessels regardless of their direction. Inspired by Fraz's
 work,²⁷ in our experiment, we set the structuring element to be 21 pixels long 1 pixel
 wide, and the element is rotated at an angle spanning $[0, 8\pi/9]$ in step of $\pi/9$. Figure 3 shows the sum of bottom-hat “ Is_{th} ”, which is the summation of the bottom-
 41 hat transformation. The set “ A ” in Eq. (6) consists of the angular orientations of
 structuring element and can be defined as $\{x | 0 \leq x \leq 8\pi/9 \& x \bmod (\pi/9) = 0\}$. As
 can be seen in Fig. 3, all vessels, including some small or tortuous vessels, can be
 enhanced by the sum of the bottom-hat on the retinal image. Besides, the bright
 zones can also be eliminated as shown in Fig. 3(c).

F. Guo et al.

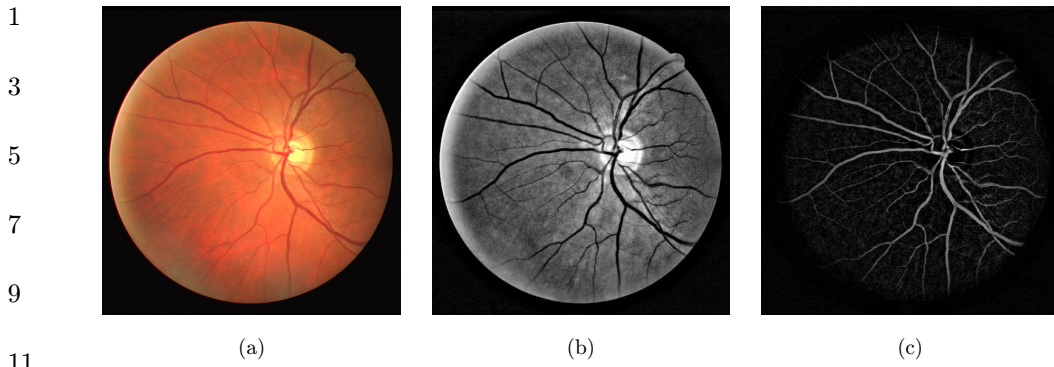


Fig. 3. Bottom-hat transformation. (a) Input retinal image. (b) Green channel of the enhanced retinal image. (c) Bottom-hat transformation result. The images in (c) are inverted for better visibility.

3.4. SIFT feature

Once the blood vessels in retinal images are segmented using the bottom-hat transformation, SIFT features are used for obtaining the local descriptor. The SIFT algorithm transforms image data into scale-invariant coordinates relative to local features and is based on four major stages: scale-space extrema detection, keypoint localization, orientation assignment and keypoint descriptor.^{14,23}

Specifically, suppose $J(x, y)$ is an input image, and its corresponding scale space is $L(x, y, \sigma)$, which can be written as

$$L(x, y, \sigma) = G(x, y, \sigma) * J(x, y), \quad (7)$$

where $*$ stands for the convolution operation, and $G(x, y, \sigma)$ is a variable-scale Gaussian function, which is defined as

$$G(x, y, \sigma) = \frac{1}{2\pi\sigma^2} e^{-(x^2+y^2)/2\sigma^2}. \quad (8)$$

In (8), (x, y) is the scale coordinate, and σ determines the smooth degree of the input image. In order to detect the stable keypoint in scale space, difference of Gaussian scale-space (DOG) is proposed. DOG detects local maxima and minima of $D(x, y, \sigma)$ by using the convolution of a difference of Gaussian with the image $J(x, y)$. This process can be written as

$$\begin{aligned} D(x, y, \sigma) &= (G(x, y, k\sigma) - G(x, y, \sigma)) * J(x, y) \\ &= L(x, y, k\sigma) - L(x, y, \sigma). \end{aligned} \quad (9)$$

To identify potential keypoints that are invariant to scale and orientation, the above operation is performed by searching over all scales and image locations. Thus, a set of keypoint candidates can be obtained. Then, the keypoints will be accurately localized. In this step, the keypoints which have low contrast or are poorly localized along an edge will be removed.

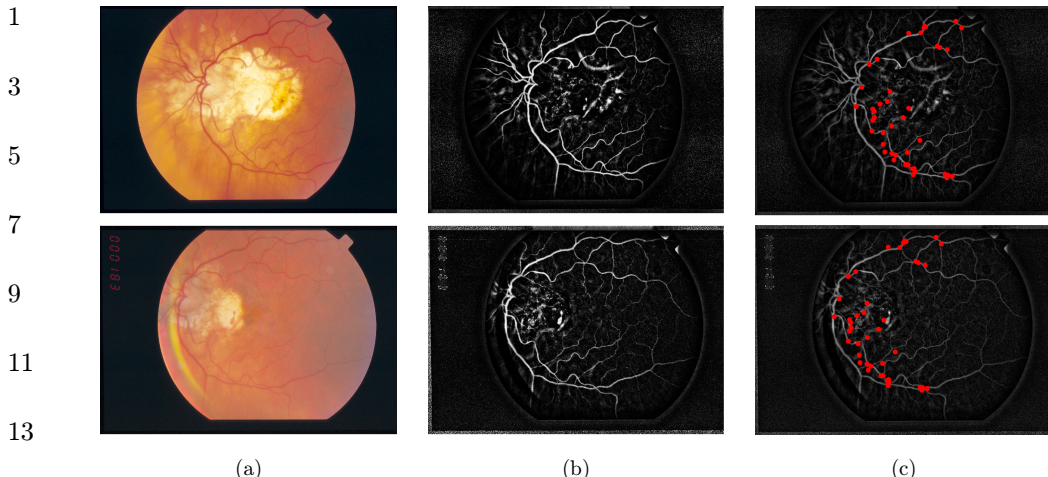
Automatic Retinal Image Registration Using Blood Vessel Segmentation and SIFT Feature

Fig. 4. SIFT keypoint extraction. (a) Input retinal images. (b) Blood vessel segmentation results. (c) Extracted SIFT keypoints.

The third step of the SIFT algorithm is assigning orientation for each keypoint. This operation is performed through an orientation histogram formed from the gradient orientations of sample points within a region around the keypoint. The histogram has 36 bins covering the 360° range of orientations. The dominant direct of the keypoint's neighborhood gradient is given by the peak of histogram, and thus the orientation histogram can be used to accurately determine the keypoint orientation.

The last stage of the SIFT algorithm is the keypoint descriptor. From the previously described steps, a K-by-4 matrix can be obtained, and each row of the matrix has the 4 values for a keypoint location (row, column, scale, orientation). The result of SIFT feature is a K-by-128 matrix, where each row gives an invariant descriptor for one of the K keypoints, and the descriptor is a vector of 128 values normalized to unit length. An illustrative example is shown in Fig. 4. As can be seen in Fig. 4(c), the keypoints of both input retinal images can be extracted by using the SIFT algorithm.

3.5. Feature matching

The main purpose of feature matching is to find the correspondences between the above features as accurate as possible, and one single method is hard to implement feature matching accurately. Therefore, the nearest neighbor method combined with the RANSAC algorithm⁹ is adopted to achieve feature matching.

Specifically, the best candidate matching for each feature points is found by using the nearest neighbor. Here, the nearest neighbor is defined as the keypoint with minimum Euclidean distance for the invariant descriptor vector. An effective measure for a matching validation is defining a ratio between the distance of the closest neighbor and the distance to the second closest neighbor. In our experiment,

F. Guo et al.

1
Table 1. The number of matched points of the proposed
3
method under R from 0.4 to 0.9.
5

	R	0.4	0.5	0.6	0.7	0.8	0.9
Proposed method	N	7	25	56	111	208	510

7 the distance ratio R is set to 0.6. To evaluate the influence of the distance ratio R used
 9 in the proposed method, some group experiments are performed by varying the distance ratio R from 0.4 to 0.9, the parameter values and the number of matched points
 11 N for a test image are presented in Table 1. For the test image, there are 1872
 13 keypoints and 1487 keypoints found in the first and second input images, respectively.
 15 The number of matched points is shown in Table 1. One can clearly see that the value
 17 range of N is [7, 510] for the proposed method when varying R from 0.4 to 0.9, which
 19 demonstrates that the influence of the distance ratio is very large in the proposed
 21 method. As can be seen in Table 1, when $R = 0.4$ or 0.5 , there are only 7 or 25 matched
 23 points, which are far from enough for feature matching. While from the keypoint
 25 matching results, we can see that when $R = 0.8$ or 0.9 , there are relatively more
 27 matching errors that interfere with the matching process. Experimental results show
 29 that when $R = 0.6$ the number of matched points is modest with the minimum of
 31 matching errors, so setting R to be 0.6 can keep a good balance between information
 33 loss and false matching. The experiments on other test images also confirm the
 35 observations.

37 However, even using the second nearest neighbor method, some matching errors
 39 still exist because of the influence from background and computation precision. To
 41 improve the precision and speed, RANSAC⁹ is used to eliminate false keypoint
 43 matching. The RANSAC algorithm is a robust transformation estimation algorithm,
 45 and it can estimate parameters of a mathematical model from a set of observed data
 47 which contains outliers. Here, the RANSAC algorithm is adopted to eliminate false
 49 matching from the SIFT keypoints. The mapping relationship of two retinal images
 51 is denoted by a homography H , which is a 3-by-3 matrix and contains the scale,
 53 rotation, and translation information of the two images. Considering the proposed
 55 algorithm mainly uses the segmented blood vessels to extract feature and the blood
 57 vessels shown in the two input retinal images belong to the adjacent areas, thus the
 59 difference caused by the retinal images that come from a somewhat spherical surface
 61 is relatively small. Besides, the experimental results also demonstrate that good
 63 registration results can be achieved by using the RANSAC algorithm. Therefore,
 65 maybe the RANSAC algorithm can be used for solving the problem of retinal image
 67 registration. Since the RANSAC algorithm is mainly for planar surface objects, we'll
 69 investigate some nonlinear models for this application in the future.

71 For the proposed registration algorithm, an illustrative example is shown in
 73 Fig. 5. In the figure, Fig. 5(a) is the keypoint matching result obtained by using SIFT
 75 algorithm for the two vessel segmentation images shown in Fig. 4(b). Figure 5(b) is
 77 the transformed image obtained by applying homography H to one of the input

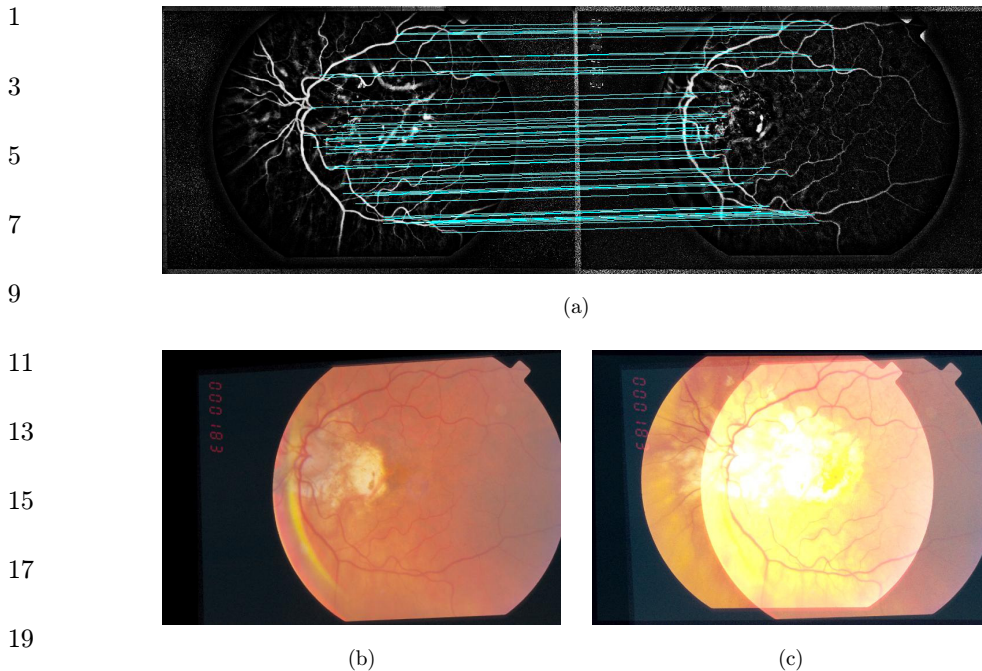
Automatic Retinal Image Registration Using Blood Vessel Segmentation and SIFT Feature

Fig. 5. Retinal image registration. (a) Keypoint matching result. (b) Transformed image obtained by applying H to the input image shown in the second row of 4(a). (c) Final registered image result.

retinal images shown in Fig. 4(a). Finally, as can be seen in Fig. 5(c), a good registered image result can be obtained.

4. Experimental Evaluation

Retinal image segmentation and registration as two difficult tasks of retinal imaging are discussed in this paper. Therefore, in this section, we first introduce the public database and the assessment indexes that used for retinal image segmentation and registration, and then the proposed method is tested on the real captured retinal images. Finally, we compared our algorithm with other methods in the literature. All the registration methods were implemented in MATLAB. The experiments were performed on a PC with 3.00 GHz Intel Pentium Dual-Core Processor.

4.1. Image segmentation evaluation

For image segmentation, the proposed method is tested on DRIVE database images^{8,40} to compare with existing works. 40 TIFF formatted RGB retinal images with a size of 565×584 pixels are included in the DRIVE database. Manually labeled retina images created by two human specialists are also contained in the database. These manually labeled images are used for comparison with the images acquired from various algorithms. Although both of the manually labeled images can be used

F. Guo et al.

1 Table 2. Vessel classification.

	Vessel Present	Vessel Absent
Vessel detected	True positive (TP)	False positive (FP)
Vessel not detected	False negative (FN)	True negative (TN)

5 Table 3. Performance indexes that used for
blood vessel segmentation.

Index	Definition
SN	$TP/(TP + FN)$
SP	$TN/(TN + FP)$
Acc	$(TP + TN)/(TP + FP + TN + FN)$

13 in comparisons, the first specialist's manual work is regard as Gold Standard just like
 many researchers' work. In binary classification, the true positive refers to any pixel
 15 which is identified as vessel by the algorithm and is also marked as vessel in the
 ground truth, while the false positive refers to any pixel which is marked as vessel in
 the segmented image but not in the ground truth image, as illustrated in Table 2.

17 The measurements used for evaluating algorithm performance are: Sensitivity
 19 (SN), Specificity (SP), and Acc.¹⁹ Table 3 shows the definition of these performance
 21 indexes that used for vessel segmentation. As can be seen in the table, SN reflects the
 23 ability of an algorithm to detect the vessel pixels. SP is the ability to detect nonvessel
 pixels. The Acc is measured by the ratio of the total number of correctly classified
 pixels (sum of true positives and true negatives) by the number of pixels in the image
 field of view (FOV).

25 We compare the performance of the proposed method with that of existing
 algorithms shown in Table 4 for the DRIVE database. The SN, SP and Acc of the
 27 proposed algorithm are compared with the results of state of the art existing
 methods. In Table 3, the performance measure of Singh,³⁸ Dai,⁶ Masoomi,²⁶
 29 Wankhede,⁴⁵ Nandy,³¹ Ceylan,³ Ding,⁷ Li²¹ are directly from their published papers.
 The Acc is one of the most important criteria for measuring the performance of vessel
 31 segmentation algorithms. As can be seen in Table 4, the proposed method renders

33 Table 4. Performance measurement for vessel segmentation methods (DRIVE
images).

No	Type	Methods	Year	SN	SP	Acc
1.	Supervised Method	Nandy ²³	2012	N.A	N.A	0.9616
2.		Ceylan ²⁴	2013	N.A	N.A	0.9856
3.		Ding ²⁵	2014	N.A	N.A	0.9120
4.		Li ²⁶	2016	0.7569	0.9816	0.9527
5.	Unsupervised Method	Dai ¹³	2013	0.6542	0.9759	0.9347
6.		Masoomi ¹⁴	2014	0.7345	0.9629	0.9425
7.		Wankhede ¹⁷	2015	0.7261	0.9806	0.9626
8.		Singh ⁷	2016	N.A	N.A	0.9522
9.	Proposed Method		2016	0.8024	0.9712	0.9562

35 Note: N.A = Not Available.

Automatic Retinal Image Registration Using Blood Vessel Segmentation and SIFT Feature

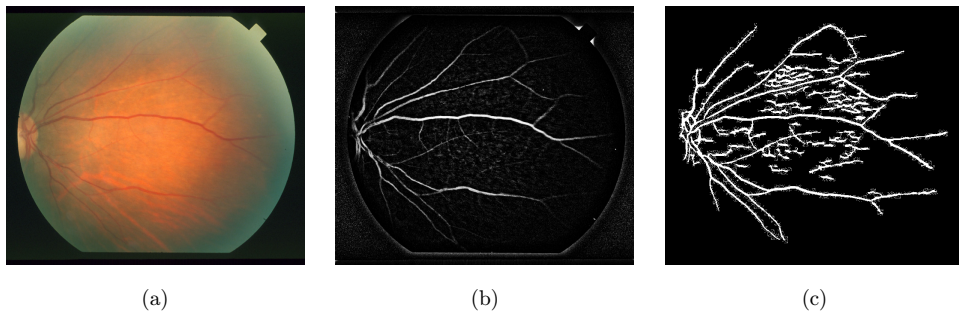


Fig. 6. Comparison of segmentation results on retinal images with uneven illumination. (a) Input image. (b) Our vessel segmentation result. (c) Soares's vessel segmentation result.

relatively better Acc than most other algorithms for the DRIVE database, and the main advantage of the method is its speed. The proposed method only takes 0.5 seconds to segment blood vessel from a retinal image with a size of 565×584 , while other existing methods utilize more computational times. For example, the segmentation algorithm with highest Acc is proposed by Ceylan *et al.*³ However, Ceylan's technique used 4th level Complex Wavelet Transform and Complex-Valued ANN for the blood vessels segmentation. Thus, the method share the common limitation of most ANN based methods — the training phase costs too much time. The same is for Li's method,²¹ and the average time required to train the deep neural network for one dataset in this method is about 7 h with an AMD Athlon II X4 645 CPU running at 3.10 GHz with 4 GB of RAM.

Besides, blood vessel segmentation also faces many challenges, such as lesions in the retinal vasculature, uneven illumination, etc. Figure 6 shows the comparison results of the segmented images in nonuniform illumination conditions. The result images that used for comparing with our method's results are downloaded from Soares' website.³⁹ One can clearly see that our blood vessel segmentation result performs better in the removal of uneven illumination areas. This can greatly reduce the incorrect pixels and provide a reliable descriptive feature for blood vessels. Thus, a good foundation for establishing pixel-to-pixel correspondence between two retinal images can be laid for the next image registration step.

4.2. Image registration evaluation

The database that is used for measuring the performance of the proposed registration algorithm is provided by the Shiley Eye Center at the University of California. The name of the database is STARE (STRUCTURED ANALYSIS OF THE RETINA), and it contains 400 retinal images with various pathologies, where each image with a size of 700×605 pixels.⁴¹ In the experiment, the blood vessels are first segmented using the segmentation method mentioned above. Then, the SIFT algorithm is applied to detect the feature of vessel segmentation images. Figures 7(a) and 7(b) are a pair of retinal images captured at different time. For this image pair, 2185 and 2476 keypoints are

F. Guo et al.

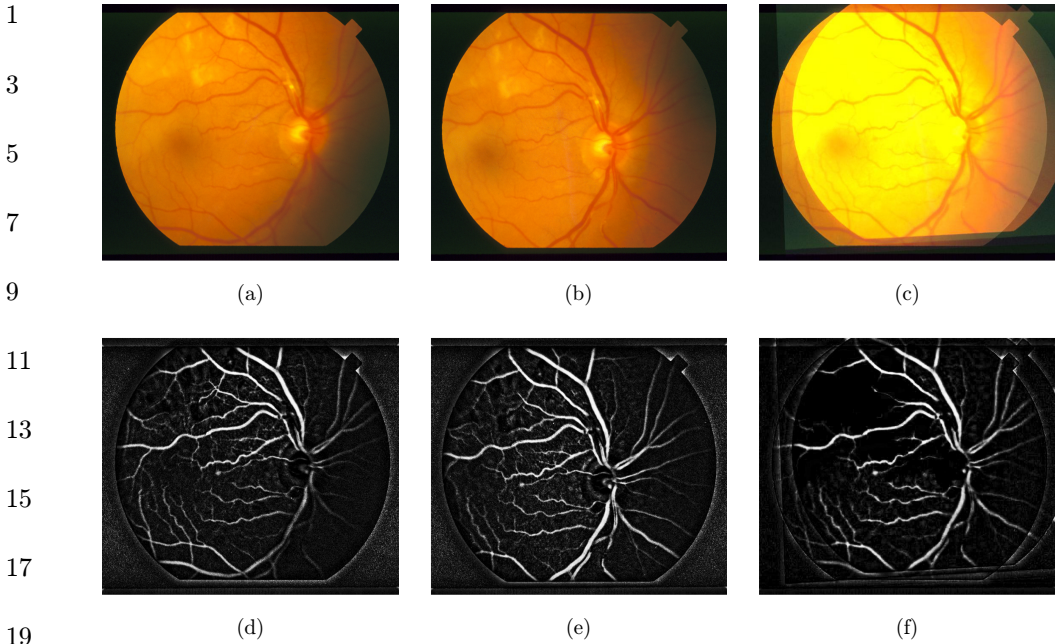


Fig. 7. Image registration result for STARE database. (a) One input retinal image. (b) Another input retinal image. (c) The image mosaic result. (d) Vessel segmentation result of (a). (e) Vessel segmentation result of (b). (f) Vessel segmentation result of the mosaic image (c).

detected and yield 139 matched pairs. The corresponding vessel segmentation results are shown in Figs. 7(d) and 7(e). To eliminate false matching from the SIFT keypoints, the RANSAC algorithm is adopted here to calculate the homography matrix H . Based on the matrix, the projective transformation is applied to implement image reprojection for the input retinal image. The mosaic image aligned by the projective transformation is shown in Figs. 7(c) and 7(f).

Another example of the registration results for image pair in the STARE database is shown in Figs. 8(a)–8(c). One can clearly see that most of the vessels are aligned

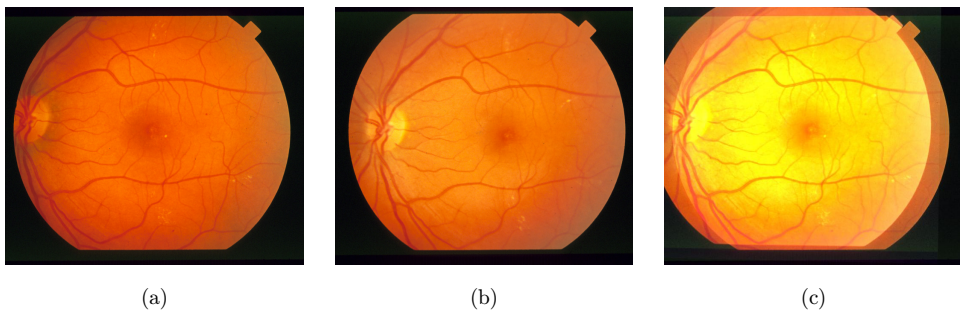


Fig. 8. Image registration result for STARE database. (a) One input retinal image. (b) Another input retinal image. (c) The image mosaic result.

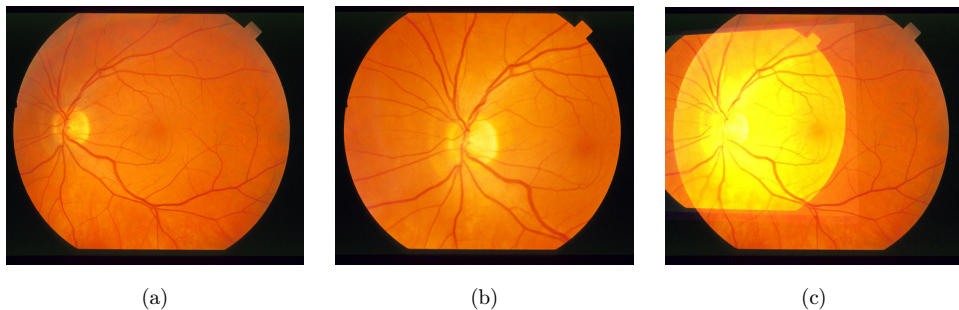
Automatic Retinal Image Registration Using Blood Vessel Segmentation and SIFT Feature

Fig. 9. Image registration result for public database. (a) One retinal image. (b) Another retinal image with different translation and scaling values. (c) The image mosaic result.

well except a few local blood vessels with a little shift. Other image pairs in the STARE database also confirm this observation, thus we can deduce that the pixel shift is caused by the failure of blood vessel segmentation in the previous operation. Therefore, the only limitation of the proposed registration algorithm is that it requires the blood vessel to be successfully segmented from the input retinal images. This constraint is common for keypoint matching registration as blood vessel detection is a prerequisite condition for retinal image registration.

Another advantage of the proposed algorithm is that it can handle translation, rotation, and scaling situation as long as the blood vessel results of image pair are available. Figures 9 and 10 show two examples of retinal image registration under such conditions. As can be seen in Fig. 9, although the two input retinal images have different translation and scaling conditions, the blood vessels are still aligned well by using the proposed algorithm, as shown in Fig. 9(c). For another example, the simulated retinal image in Fig. 10(c) is obtained by 90° rotation and 0.9 down-sampling of Fig. 10(b). The SIFT algorithm combined with the RANSAC algorithm is used to find the correct matches between Figs. 10(a) and 10(c). The mosaic retinal image in Fig. 10(d) clearly demonstrates the effectiveness of the proposed algorithm in dealing with vasculature-like pattern registration.

4.3. Real captured retinal image test

The algorithm proposed in this paper also works well for a wide variety of real captured retinal images. In our experiments, the TOPCON TRC-NW400 non-mydriatic fundus camera is used to collect fundus images. Some of the input image pairs were taken at the same time with different viewpoints, while others were taken at different time (e.g. a few days or months later). The minimum overlapping area of viewpoint image pairs is approximately 40%. The test was performed by 36 subjects. The subjects were chosen from among voluntary undergraduate and graduate students. The total number of collected image pairs is 82, and the size of each test image is 1956×1934 .

F. Guo et al.

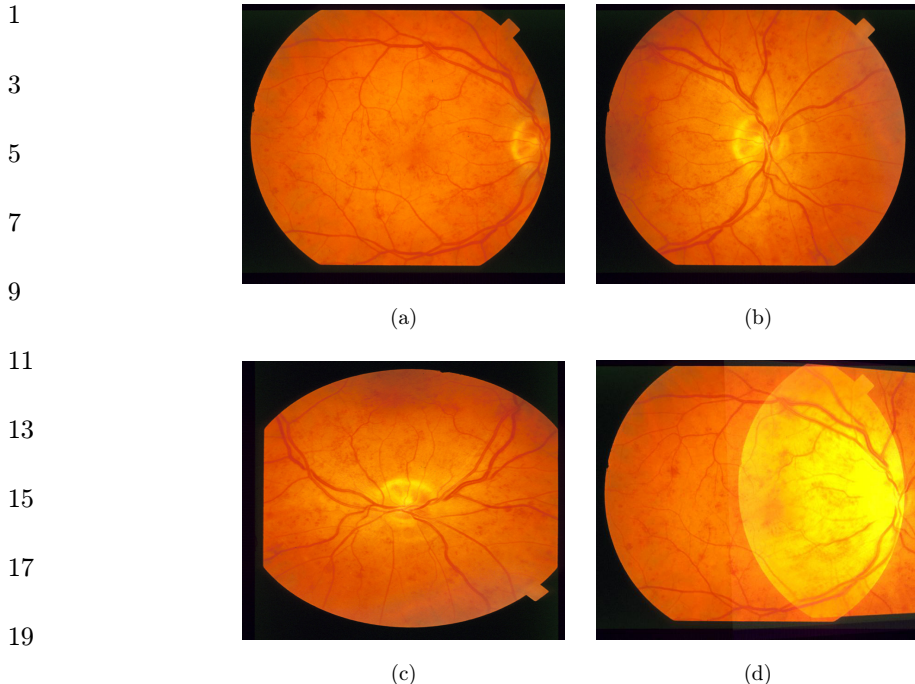


Fig. 10. Image registration result for public database. (a) One input retinal image. (b) Another input retinal image. (c) Simulated retinal image obtained using translation, rotation and scaling operation to (b). (d) The mosaic result obtained using (a) and (c).

Figure 11 shows some examples of image registration results for the real captured images captured by fundus camera. The captured image pairs have 45% and 65% overlapping areas, respectively. To test the rotation invariant performance of the proposed method, the first image is held fix and the second image is rotated by 180° and 90°, respectively, as shown in Fig. 11(c). We applied the proposed method on the first image and the rotating second image. As can be seen in the figure, the proposed method can successfully mosaic these images pairs regardless of the rotation angle. This demonstrates that our method is rotation invariant. Besides, since it is rare to capture retinal images with both small overlapping and large scale change in clinical applications, the proposed method is thus tested on the real captured image pairs with the 50% overlapping areas and the second image is rescaled by 0.85 down-sampling. Experimental results show that our algorithm is still suitable for retinal image registration in this situation.

The real captured images with noise are also used to verify the effectiveness of the proposed method. Noise in retinal image is normally due to noise pixels and pixels whose color is distorted.¹⁶ The former noise pixels refer to the pixel that affected by various types of noises such as Gaussian noise and Multiplicative noise, and the latter color distorted pixels seem to exist in regions where illumination has been inadequate. Therefore, in our experiments, the noisy retinal images with Gaussian noise

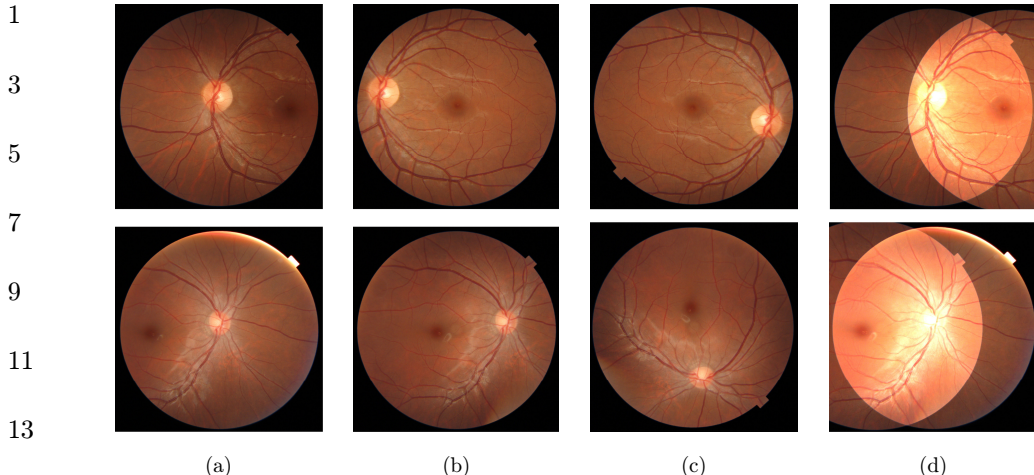
Automatic Retinal Image Registration Using Blood Vessel Segmentation and SIFT Feature

Fig. 11. Image registration results for real captured images. (a) and (b) are two captured retinal images. (c) The rotating images for (b) (the rotation angle of the top row is 180° and that of the bottom row is 90°). (d) The image mosaic results.

and Multiplicative noise are first tested, and then the fundus images with low illumination are also selected to evaluate the robustness of the proposed method.

Figure 12 shows an example of image registration with different noise. The Gaussian noise with a variance of 0.001 and the Multiplicative noise with a variance of 0.01 are added on the two input images, respectively. One can clearly see that the proposed method can still obtain a good keypoint matching and image mosaic results

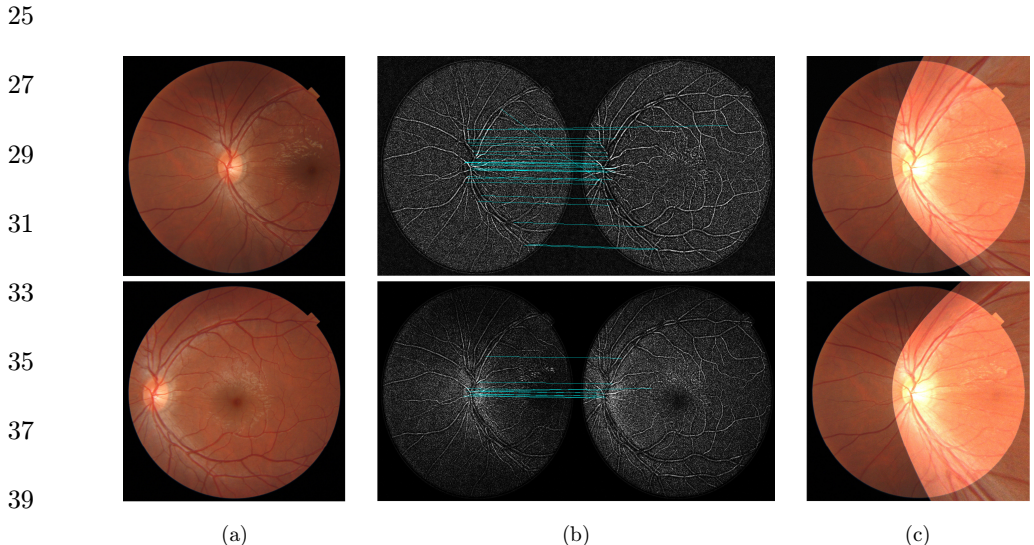


Fig. 12. Image registration results for the real captured images with Gaussian noise and Multiplicative noise. (a) The two input retinal images. (b) The keypoint matching results for different noise (top: result for Gaussian noise, bottom: result for Multiplicative noise). (c) The corresponding image mosaic results.

F. Guo et al.

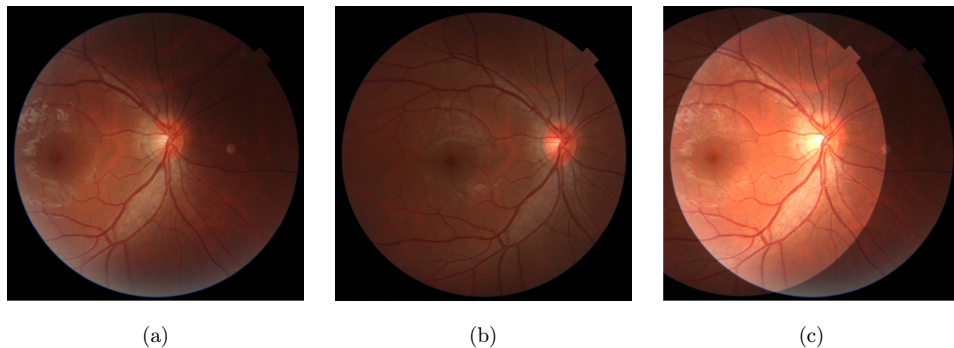


Fig. 13. Image registration results for the real captured images with low illumination. (a) and (b) are two input retinal images with low illumination. (c) The image mosaic results.

even with those noises. However, if the added noise is too strong (e.g. the variance of Gaussian noise is set to 0.05), the proposed method may fail in this situation. Thus, we can deduce that the proposed method can deal well with slight noise. The image registration results for the real captured images with low illumination are shown in Fig. 13. The mosaic result supports the validity of our technique and show that our technique gives good results for the noisy areas caused by inadequate illumination. Since most retinal images captured by fundus camera in clinical practice usually have a clear visual effect with little noise and adequate illumination. Thus, our method is suitable for retinal image registration.

4.4. Comparative study

Some representative retinal image registration algorithms were compared, such as bifurcation structure method⁴ and region detector method¹³ with our proposed method. The reasons for choosing the above two image registration methods were that the former is one of the representative structure-matching methods, and the latter is one of the representative region-matching methods. Therefore, we choose the above two methods for comparison with our proposed point-matching method. However, in our experiment, we find that there is no method can solve all problems, and each kind of method has its own drawbacks.

For the bifurcation structure method,⁴ bifurcation extraction requires reliable centerline detection of vessels. However, the assumption that the vessel centerlines should be given limits its use in real applications. Figuer 14 shows the image registration result for the two input retinal images presented in Fig. 4(a) by using the bifurcation structure method. Figures 14(a) and 14(b) are the corresponding topological vascular trees for the two input images that are assumed to be given. The mosaic vessel image is shown in Fig. 14(c), and the two input images can be registered based on the mosaic vessel image, as shown in Fig. 14(d). Our proposed method doesnot need any prior or reference information in advance. The proposed algorithm first automatically segments blood vessel and then mosaics the two input images

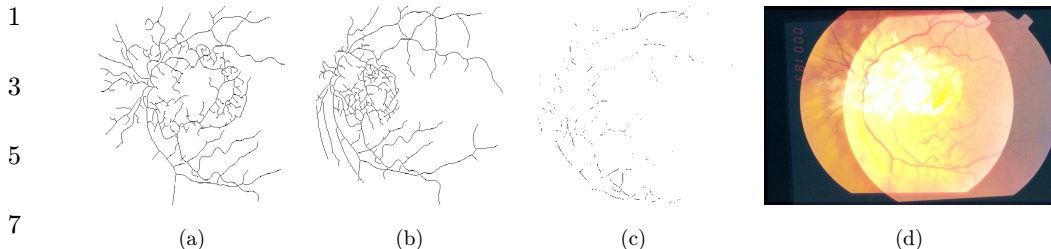
Automatic Retinal Image Registration Using Blood Vessel Segmentation and SIFT Feature

Fig. 14. Image registration result of the bifurcation structure method for the two input retinal images shown in Fig. 4(a). (a) and (b) are the topological vascular trees for the input images shown in Fig. 4(a). (c) The mosaic vessel image. (d) The mosaic retinal image.

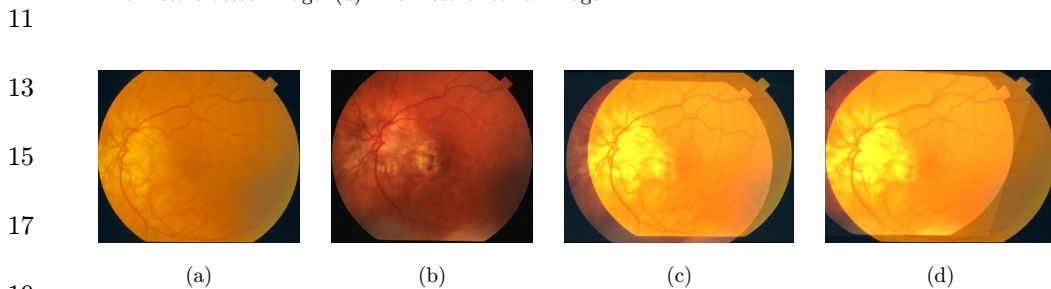


Fig. 15. Comparison between the registration results of the bifurcation structure method and the proposed method. (a) One input retinal image. (b) Another input retinal image. (c) Registration result obtained using bifurcation structure method. (d) Registration result obtained by the proposed method.

based on the segmented vessels. As can be seen in Fig. 5(c), similar registration result can be obtained without any user-interaction by using the proposed method.

Another illustrative example is shown in Fig. 15. One can clearly see that comparable mosaic results can be obtained by the proposed algorithm. Observation on other test images also confirms this conclusion. However, for an image pair with each image size of 689×471 , the running time of the bifurcation structure method is more than 5 s even if the vessel centerlines are previously given, and our method needs about 4 s on average to automatically register the image pair.

For the region detector method,¹³ the main advantage is its speed. The method only takes about 30 s to register an image pair with each image size of 2048×1536 , which is faster than the proposed algorithm. However, the region detector method involves many parameters that need to be manually tuned according to different input images to ensure a good mosaic result. These parameters include the minimum and maximum scales at which the vessels are expected to be found, the number of pixels that are regarded as the small regions in watershed transform, the ratio between the first and second minimum distance in region matching, and the number of match points that used for selecting a model type, etc. Our proposed algorithm is controlled only by a parameter, and the experimental results demonstrate that similar or better quality results are obtained, as shown in Figs. 16(c) and 16(d).

F. Guo et al.

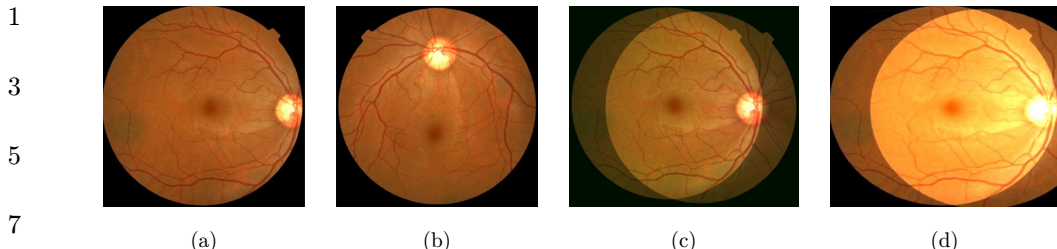
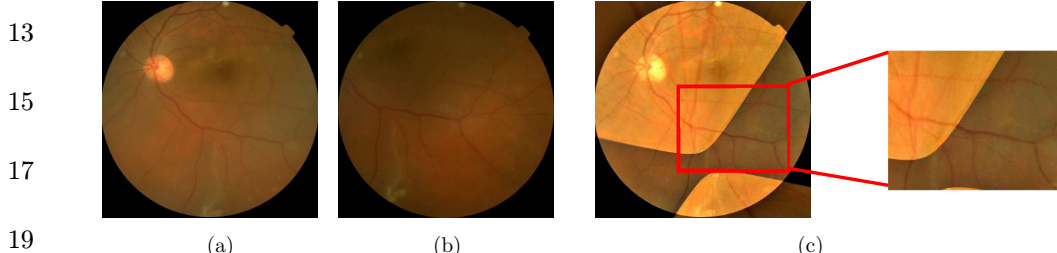


Fig. 16. Comparison between the registration results of the region detector method and the proposed method. (a) One input retinal image. (b) Another input retinal image. (c) Registration result obtained using region detector method. (d) Registration result obtained by the proposed method.

11



21

Fig. 17. Our registration result for an image pair that has not been registered by the region detector method. (a) One input retinal image. (b) Another input retinal image. (c) Registration result obtained by the proposed method.

23

25

Besides, the region detector method may also fail in the presence of low-quality images.¹³ Figure 17 shows such image pair. The second retinal image is blurred due to the lens problems of the eyes. In this situation, the region detector method is unable to provide a reliable vascular structure map for the stable region detection. That's because the method is based on a watershed segmentation of a clean vascular structure map to detect polygonal regions and the segmentation will fail when the input image is blur. On the contrast, thanks to the guided filter that is used for enhancing the details of the input images in the preprocessing stage, our proposed method is able to register the image pair. Figure 17(c) shows the registration result obtained by our method. As can be seen in the figure, our algorithm is able to deal with the challenge of image blur.

35

37

5. Discussion and Conclusion

39

In this section, we first discuss some critical issues, such as technique challenges, limitations, and possible solutions that relate to the technique contribution of the proposed method.

41

Two fundamental tasks of retinal image analysis (image segmentation and registration) are discussed in this paper. Since the only limitation of the proposed registration algorithm is that it requires the blood vessel to be successfully segmented

Automatic Retinal Image Registration Using Blood Vessel Segmentation and SIFT Feature

from the input retinal image, thus the blood vessel segmentation is very important for the proposed method. However, this issue faces many technique challenges: (a) the presence of lesions and strong noise; (b) uneven illumination; (c) drift in intensity; (d) lack of image contrast between background and vessel regions; (e) varying vessel width; (f) central vessel reflex. Although some measures have been taken to solve a part of the above problems using unsupervised or supervised schemes, the proposed segmentation method shows comparative performance against other algorithms in terms of speed and effect. However, the proposed segmentation method also has some limitations. For example, the bottom-hat transformation result is chosen as the extracted feature for image segmentation. In the experiment, we find that although most of the vessels are aligned well in this way, there still exist a few local blood vessels with a little shift. Nevertheless, we provide a new way to solve the problem of blood vessel segmentation, which is quite essential for automatic retinal image registration.

Once the blood vessel is segmented by using the guided filter and bottom-hat transformation, the SIFT algorithm is adopted to detect the features of the vessel segmentation image, and the RANSAC algorithm is also used to eliminate some error matches. The proposed registration method can deal with both normal and pathological retinas. To verify the effectiveness of the proposed algorithm, we test the method on the public database and real captured retinal images. The demonstrated performance, effectiveness and robustness along with its simplicity in retinal image segmentation as well as in registration, make the proposed method a suitable tool to be integrated into a retinal image analysis system for clinical purposes. Therefore, many practical applications in the medical field can benefit from the proposed method.

In the future, we intend to investigate the following possible solutions to enhance the flexibility of the proposed registration algorithm: (a) incorporating the vessel width and tortuosity measures into the vessel segmentation method; (b) choosing more proper feature vector and nonlinear model to improve the efficiency and Acc of the retinal image registration; (c) further minimizing the computation times to meet the needs of practical requirements; (d) developing an interactive image registration software tool for ophthalmologists; (e) testing our algorithm on larger image databases and cooperating with clinical partners.

33 Acknowledgment

35 This work was supported in part by the National Natural Science Foundation of
36 China (Nos. 61502537 and 61573380), Natural Science Foundation of Hunan
37 Province, China (No. 14JJ2008), and Postdoctoral Science Foundation of Central
38 South University (No. 126648).

39

41 References

1. B. Al-Diri, A. Hunter and D. Steel, An active contour model for segmenting and measuring retinal vessels, *IEEE Trans. Med. Imaging* **28**(9) (2009) 1488–1497.

F. Guo et al.

- 1 2. E. Aswini, S. Divya, S. Kardheepan and T. Manikandan, Mathematical morphology and
bottom-hat filtering approach for crack detection on relay surfaces, in *Proc. IEEE Int.
Conf. Smart Structures and Systems* (2013), pp. 108–113.
- 3 3. M. Ceylan and H. Yasar, Blood vessel extraction from retinal images using complex
wavelet transform and complex-valued artificial neural network, in *Proc. 36th Int. Conf.
Telecommunications and Signal Processing* (2013), pp. 822–825.
- 5 4. L. Chen, X. T. Huang and J. Tian, Retinal image registration using topological vascular
tree segmentation and bifurcation structures, *Biomed. Signal Proc. Control* **16** (2015)
22–31.
- 7 5. L. Chen, Y. Xiang, Y. J. Chen and X. L. Zhang, Retinal image registration using bifur-
cation structures, in *Proc. 18th IEEE Int. Conf. Image Process.* (2011), pp. 2169–2172.
- 9 6. B. S. Dai, W. Bu, X. Q. Wu and Y. L. Zheng, Retinal blood vessel detection using
multiscale line filter and phase congruency, in *Proc. Int. Conf. Image Processing,
Computer Vision & Pattern Recognition* (2013), pp. 1–7.
- 11 7. C. Ding, Y. Xia and Y. Li, Supervised segmentation of vasculature in retinal images using
neural networks, in *Proc. IEEE Int. Conf. Orange Technologies* (2014), pp. 49–52.
- 13 8. DRIVE database [Online]. Available: <http://www.isi.uu.nl/Research/Databases/DRIVE>.
- 15 9. M. A. Fischler and R. C. Bolles, Random sample consensus: A paradigm for model fitting
with applications to image analysis and automated cartography, *Commun. ACM* **24**(6)
(1981) 381–395.
- 17 10. A. F. Frangi, W. J. Niessen, K. L. Vincken and M. A. Viergever, Multiscale vessel en-
hancement filtering, *Med. Image Comput. Comput. Assist. Interv.* (1496) 130–137.
- 19 11. M. M. Fraz, S. A. Barman, P. Remagnino, A. Hoppe, A. Basit, B. Uyyanonvara, A. R.
Rudnickc and C. G. Owen, An approach to localize the retinal blood vessels using bit planes
and centerline detection, *Comput. Methods Programs Biomed.* **108**(2) (2012) 600–616.
- 21 12. M. M. Fraz, P. Remagnino, A. Hoppe, B. Uyyanonvara, A. R. Rudnicka, C. G. Owen and
S. A. Barman, An ensemble classification-based approach applied to retinal blood vessel
segmentation, *IEEE Trans. Biomed. Eng.* **59**(9) (2012) 2538–2548.
- 23 13. Z. Ghassabi, J. Shanbehzadeh and A. Mohammadzadeh, A structure-based region de-
tector for high-resolution retinal fundus image registration, *Biomed. Signal Process.
Control* **23** (2016) 52–61.
- 25 14. H. Goncalves, L. Corte-Real and J. A. Goncalves, Automatic image registration through
image segmentation and SIFT, *IEEE Trans. Geosci. Remote Sensing* **49**(7) (2011)
2589–2600.
- 27 15. K. M. He, J. Sun and X. O. Tang, Guided image filtering, *IEEE Trans. Pattern Anal.
Mach. Intell.* **35**(6) (2013) 1397–1409.
- 29 16. I. Jamal, M. U. Akram and A. Tariq, Retinal image preprocessing: Background and noise
segmentation, *TELKOMNIKA* **10**(3) (2012) 537–544.
- 31 17. Y. Keller, A. Averbuch and M. Israeli, Pseudo polar-based estimation of large transla-
tions, rotations, and scalings in images, *IEEE Trans. Image Process.* **14**(1) (2005) 12–22.
- 33 18. C. Kirbas and F. Quek, A review of vessel extraction techniques and algorithms, *ACM
Comput. Surv.* **36**(2) (2002) 81–121.
- 35 19. F. Laliberté, L. Gagnon and Y. L. Sheng, Registration and fusion of retinal images — an
evaluation study, *IEEE Trans. Med. Imaging* **22**(5) (2003) 661–673.
- 37 20. B. S. Y. Lam, G. Yongsheng and A. W. C. Liew, General retinal vessel segmentation using
regularization-based multiconcavity modeling, *IEEE Trans. Med. Imaging* **29**(7) (2010)
1369–1381.
- 39 21. Q. L. Li, B. W. Feng, L. P. Xie, P. Liang, H. S. Zhang and T. F. Wang, A cross-modality
learning approach for vessel segmentation in retinal images, *IEEE Trans. Med. Imaging*
35(1) (2016) 109–118.

Automatic Retinal Image Registration Using Blood Vessel Segmentation and SIFT Feature

- 1 22. Q. L. Li, H. S. Zhang and T. F. Wang, Scale invariant feature matching using rotation-
3 invariant distance for remote sensing image registration, *Int. J. Pattern Recognit. Artif. Intell.* **27**(2) (2013) 1–18.
5 23. D. G. Lowe, Distinctive image features from scale-invariant keypoints, *Int. J. Comput. Vis.* **60**(2) (2004) 91–110.
7 24. J. B. A. Maintz and M. A. Viergever, A survey of medical image registration, *Med. Image Anal.* **2**(1) (1998) 1–36.
9 25. M. S. Makrouk, N. H. Solouma and Y. M. Kadah, Survey of retinal image segmentation and registration, *Int. J. Graphics Vision Image Process.* **6**(2) (2006) 1–11.
11 26. R. Masoomi, A. Ahmadifard and A. Mohtadizadeh, Retinal vessel segmentation using non-subsampled contourlet transform and multi-scale line detection, in *Proc. Iranian Conference on Intelligent Systems* (2014), pp. 1–5.
13 27. G. K. Matsopoulos, P. A. Asvestas, N. A. Mouravliansky and K. K. Delibasis, Multimodal registration of retinal images using self-organizing maps, *IEEE Trans. Med. Imaging* **23**(12) (2004) 1557–1563.
15 28. G. K. Matsopoulos, N. A. Mouravliansky, K. K. Delibasis and K. S. Nikita, Automatic retinal image registration scheme using global optimization techniques, *IEEE Trans. Inf. Technol. Biomed.* **3**(1) (1999) 47–60.
17 29. A. M. Mendonca and A. Campilho, Segmentation of retinal blood vessels by combining the direction of centerlines and morphological reconstruction, *IEEE Trans. Med. Imaging* **25**(9) (2006) 1200–1213.
19 30. K. Mikolajczyk and C. Schmid, A performance evaluation of local descriptors, *IEEE Trans. Pattern Anal. Mach. Intell.* **27**(10) (2005) 1615–1630.
21 31. M. Nandy and M. Banerjee, Retinal vessel segmentation using Gabor filter and artificial neural network, in *Proc. Third Int. Conf. Emerging Applications of Information Technology* (2012), pp. 157–160.
23 32. M. Niemeijer, J. Staal, B. van Ginneken, M. Loog and M. D. Abramoff, Comparative study of retinal vessel segmentation methods on a new publicly available database, *Proc. SPIE* **5370** (2004) 648–665.
25 33. S. S. Patankar and J. V. Kulkarni, Orthogonal moments for determining correspondence between vessel bifurcations for retinal image registration, *Comput. Methods Programs Biomed.* **119**(3) (2015) 121–141.
27 34. G. P. Penney, J. Weese, J. A. Little, P. Desmedt, D. L. G. Hill and D. J. Hawkes, A comparison of similarity measures for use in 2-D–3-D medical image registration, *IEEE Trans. Med. Imaging* **17**(4) (1998) 586–595.
29 35. F. K. H. Quek and C. Kirbas, Vessel extraction in medical images by wave-propagation and traceback, *IEEE Trans. Med. Imaging* **20**(2) (2001) 117–131.
31 36. E. Ricci and R. Perfetti, Retinal blood vessel segmentation using line operators and support vector classification, *IEEE Trans. Med. Imaging* **26**(10) (2007) 1357–1365.
33 37. N. Ritter, R. Owens, J. Cooper, R. H. Eikelboom and P. P. van Saarloos, Registration of stereo and temporal images of the retina, *IEEE Trans. Med. Imaging* **18**(5) (1999) 404–418.
35 38. N. P. Singh and R. Srivastava, Retinal blood vessels segmentation by using Gumbel probability distribution function based matched filter, *Comput. Methods Programs Biomed.* **129** (2016) 40–50.
37 39. Soares’s website [Online]. Available: <http://www.ces.clemson.edu/~ahoover/stare/probing/index.html/>.
39 40. J. Staal, M. D. Abramoff, M. Niemeijer, M. A. Viergever and B. van Ginneken, Ridge-based vessel segmentation in color images of the retina, *IEEE Trans. Med. Imaging* **23**(4) (2004) 501–509.

F. Guo et al.

- 1 41. STARE database [Online]. Available: <http://www.ces.clemson.edu/~ahoover/stare/>.
- 2 42. K. W. Sum and P. Y. S. Cheung, Vessel extraction under non-uniform illumination: A
3 level set approach, *IEEE Trans. Biomed. Eng.* **55**(1) (2008) 358–360.
- 4 43. D. Tell and S. Carlsson, Combining appearance and topology for wide baseline matching,
5 in *Proc. European Conf. Computer Vision* (2002), pp. 68–81.
- 6 44. G. Wang, Z. C. Wang, Y. F. Chen, Q. Q. Zhou and W. D. Zhao, Removing mismatches
7 for retinal image registration via multi-attribute-driven regularized mixture model, *Inf.
Sci.* **372** (2016) 492–504.
- 8 45. P. R. Wankhede and K. B. Khanchandani, Retinal blood vessel segmentation using graph
9 cut analysis, in *Proc. Int. Conf. Industrial Instrumentation and Control* (2015), pp. 1429–
1432.
- 10 46. X. You, Q. Peng, Y. Yuan, Y. Cheung and J. Lei, Segmentation of retinal blood vessels
11 using the radial projection and semi-supervised approach, *Pattern Recognit.* **44** (2011)
12 2314–2324.
- 13 47. F. Zana and J. C. Klein, A multimodal registration algorithm of eye fundus images using
14 vessels detection and Hough transform, *IEEE Trans. Med. Imaging* **18**(5) (1999)
15 419–428.
- 16 48. F. Zana and J. C. Klein, Segmentation of vessel-like patterns using mathematical mor-
17 phology and curvature evaluation, *IEEE Trans. Image Process.* **10**(7) (2001) 1010–1019.



Fan Guo received the B.S. degree in Computer Science and Technology from Central South University (CSU), Changsha, China, in 2005, and the M.S. degree and the Ph.D. degree in computer application technology from CSU, Changsha, China, in 2008 and 2012, respectively. Currently, she is a Lecturer with the School of Information Science and Engineering, CSU. Her main research interests include image processing, pattern recognition and virtual reality.



Xin Zhao received the B.S. degree from University of South China, Hengyang, China, in 2017. Currently, he is pursuing the M.S. degrees at the school of Information Science and Engineering in Central South University, Changsha, China. His main research interests include image processing, pattern recognition.

31

33

35

37

39

41